REPORT

A Syndromic Neurodevelopmental Disorder Caused by De Novo Variants in *EBF3*

Hsiao-Tuan Chao,[1,2,13] Mariska Davids,[3,13] Elizabeth Burke,[4] John G. Pappas,[5] Jill A. Rosenfeld,[6] Alexandra J. McCarty,[3] Taylor Davis,[4] Lynne Wolfe,[3,4] Camilo Toro,[3,4] Cynthia Tifft,[3,4] Fan Xia,[6,7] Nicholas Stong,[8] Travis K. Johnson,[9] Coral G. Warr,[9] Undiagnosed Diseases Network, Shinya Yamamoto,[2,6,10,11] David R. Adams,[3,4] Thomas C. Markello,[3,4] William A. Gahl,[3,4] Hugo J. Bellen,[2,6,10,11,12] Michael F. Wangler,[2,6,11,*] and May Christine V. Malicdan[3,4,*]

Early B cell factor 3 (*EBF3*) is a member of the highly evolutionarily conserved Collier/Olf/EBF (COE) family of transcription factors. Prior studies on invertebrate and vertebrate animals have shown that EBF3 homologs are essential for survival and that loss-of-function mutations are associated with a range of nervous system developmental defects, including perturbation of neuronal development and migration. Interestingly, aristaless-related homeobox (ARX), a homeobox-containing transcription factor critical for the regulation of nervous system development, transcriptionally represses *EBF3* expression. However, human neurodevelopmental disorders related to *EBF3* have not been reported. Here, we describe three individuals who are affected by global developmental delay, intellectual disability, and expressive speech disorder and carry de novo variants in *EBF3*. Associated features seen in these individuals include congenital hypotonia, structural CNS malformations, ataxia, and genitourinary abnormalities. The de novo variants affect a single conserved residue in a zinc finger motif crucial for DNA binding and are deleterious in a fly model. Our findings indicate that mutations in *EBF3* cause a genetic neurodevelopmental syndrome and suggest that loss of *EBF3* function might mediate a subset of neurologic phenotypes shared by *ARX*-related disorders, including intellectual disability, abnormal genitalia, and structural CNS malformations.

An estimated 7.6 million children are born annually with congenital neurodevelopmental disorders, encompassing several clinically and biologically heterogeneous conditions including intellectual disability, autism spectrum disorder (ASD), and epilepsy.[1–3] The underlying disease-causing mechanism remains elusive when a genetic disorder lacks strong unique features to stratify the affected individuals for traditional phenotypically driven gene discovery. The advent of whole-exome sequencing (WES) has provided a powerful tool for discovering disease-associated genes by identifying mutations in a population of individuals presenting with rather non-specific clinical features.[4–6]

We have identified three individuals with a previously unrecognized genetic syndromic disorder characterized by global developmental delay (3/3), hypotonia (3/3), intellectual disability (3/3), mild facial dysmorphisms (3/3), facial weakness (3/3), expressive speech disorder (3/3), ataxia (3/3), perseverative social behaviors (1/3), motor stereotypies (1/3), decreased pain response (2/3), structural CNS malformations (2/3), and genitourinary malformations (2/3) (Figure 1 and Table S1). These three individuals all have de novo *EBF3* (MIM: 607407; HGNC: 19087) missense variants that affect the same amino acid residue (Arg163) in the Zn^{2+} finger Collier/Olf/Ebf (COE) motif and are predicted to be putatively deleterious by SIFT and PolyPhen-2 models (Figure 1A and Table S2). The coincidental occurrence of three de novo variants affecting the same residue in individuals with similar phenotypes from a total WES cohort of 7,595 individuals is highly unlikely and remains statistically significant after correction for the size of the targeted exome ($p = 2.1 \times 10^{-3}$).[7–9] Prior statistical models examining observed versus expected functional coding variation revealed that *EBF3* undergoes selective restraint, a process where selection has reduced functional variation, suggesting that mutations are more likely to be deleterious.[10,11] Statistical analysis comparing the observed to the expected functional variation across the genome for *EBF3* resulted in a Residual Variation Intolerance Score (RVIS) of −0.646, where RVIS < 0 indicates that there is less common functional variation than predicted.[10] Furthermore, in a model of de novo mutations for ASD and intellectual disability, the statistical analysis identified *EBF3* as one of ~1,000 genes that significantly lack functional variation in non-ASD individuals but are enriched with de novo loss-of-function mutations in affected individuals.[11] Similarly, analysis of the ExAC (Exome Aggregation Consortium) Browser revealed that

[1]Section of Child Neurology, Department of Pediatrics, Baylor College of Medicine, Houston, TX 77030, USA; [2]Jan and Dan Duncan Neurological Research Institute, Texas Children's Hospital, Houston, TX 77030, USA; [3]Undiagnosed Diseases Program, NIH Common Fund, Office of the Director, National Human Genome Research Institute, NIH, Bethesda, MD 20892, USA; [4]Office of the Clinical Director, National Human Genome Research Institute, NIH, Bethesda, MD 20892, USA; [5]Department of Pediatrics, New York University Langone Medical Center, New York, NY 10016, USA; [6]Department of Molecular and Human Genetics, Baylor College of Medicine, Houston, TX 77030, USA; [7]Baylor Genetics Laboratories, Houston, TX 77030, USA; [8]Institute for Genomic Medicine, Columbia University, New York, NY 10032, USA; [9]School of Biological Sciences, Monash University, Melbourne, VIC 3800, Australia; [10]Department of Neuroscience, Baylor College of Medicine, Houston, TX 77030, USA; [11]Program in Developmental Biology, Baylor College of Medicine, Houston, TX 77030, USA; [12]Howard Hughes Medical Institute, Baylor College of Medicine, Houston, TX 77030, USA
[13]These authors contributed equally to this work
*Correspondence: mw147467@bcm.edu (M.F.W.), maychristine.malicdan@nih.gov (M.C.V.M.)
http://dx.doi.org/10.1016/j.ajhg.2016.11.018.

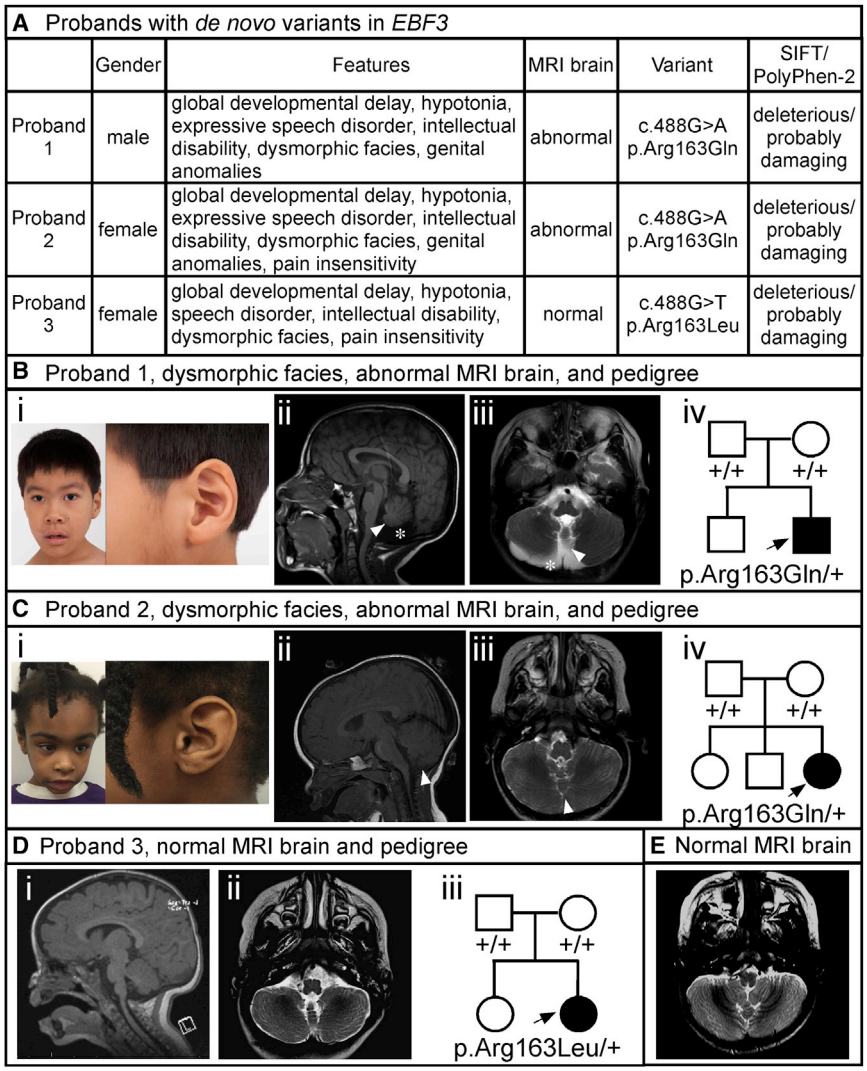

Figure 1. Probands and Phenotypic Features

(A) Summary of phenotypic features, brain MRI findings, gene variants, and SIFT and PolyPhen-2 predictions for the three probands with the de novo EBF3 p.Arg163Gln and p.Arg163Leu variants.

(B) Proband 1. Representative images show (i) mild facial dysmorphisms including oval-shaped myopathic facies, short anteverted nostrils, and overfolding of the superior helices, (ii) mid-sagittal T1-weighted and (iii) axial T2-weighted images depicting vermian hypoplasia (white arrows) and reduced cerebellar hemispheres volume (white asterisk), and (iv) a pedigree showing the de novo p.Arg163Gln variant.

(C) Proband 2. Representative images show (i) mild facial dysmorphisms including triangular myopathic facies and overfolding of the superior helices, (ii) mid-sagittal T1-weighted and (iii) axial T2-weighted images depicting vermian hypoplasia (white arrows) with normal cerebellar hemispheres, and (iv) a pedigree showing the de novo p.Arg163Gln variant.

(D) Proband 3. Brain MRI shows (i) mid-sagittal T1-weighted and (ii) axial T2-weighted images depicting normal cerebellar vermis and hemispheres. A pedigree (iii) shows the de novo p.Arg163Leu variant.

(E) A representative axial T2-weighted image from the normal brain MRI of a 23-month-old control individual is shown for comparison. Note the typical cerebellar hemispheres and vermian structures.

EBF3 has a high probability of loss-of-function intolerance (pLI = 1.0), given that 23.2 loss-of-function variants were expected given the gene's size and GC content but only one loss-of-function variant was observed.[12] Together, these statistical findings provide strong evidence that the recurrent de novo variants in *EBF3* cause the observed neurodevelopmental disorder.

Clinical data were obtained after written informed consent was provided and procedures were followed in accordance with the ethical standards of the participating institutional review boards on human research and in keeping with national standards. The NIH Undiagnosed Diseases Program (UDP) under protocol 76-HG-0238, "Diagnosis and Treatment of Patients with Inborn Errors of Metabolism or Other Genetic Disorders," approved by the National Human Genome Research Institute Institutional Review Board, identified a de novo c.488G>A (p.Arg163Gln) missense change in *EBF3* (GenBank: NM_001005463.2) for proband 1 by exome sequencing (Supplemental Note and Table S3). Sequence changes c.488G>A (p.Arg163Gln) and c.488G>T (p.Arg163Leu) were identified for probands 2 and 3, respectively, by clinically based exome sequencing performed in the Baylor Genetics Laboratory, certified by the Clinical Laboratory Improvement Amendments (Supplemental Note and Table S3). Sanger sequencing of the parental samples to confirm segregation revealed de novo variants for all three probands. Paternity was confirmed by the inheritance of rare SNPs from the parents. Sample swap was excluded. Neither of the changes is present in the ExAC Browser.[12] The clinical phenotypes of these individuals and their *EBF3* variants are depicted in Figure 1, described in the Supplemental Note, and summarized below.

Proband 1 is a 7-year-old male Pacific Islander of Chinese and Japanese descent and has a de novo c.488G>A (p.Arg163Gln) missense change in *EBF3*. No significant findings were revealed during previous targeted genetic testing, karyotype analysis, or chromosomal microarray analysis; SNP array analysis showed no anomalous regions of homozygosity or significant copy-number variants (CNVs). His prenatal history is significant for decreased fetal movements, and he was born at full term at 38 weeks of gestation by caesarean section with a birth weight of 3.4 kg (25^{th}–50^{th} percentile). His clinical features include

congenital hypotonia, facial weakness, global developmental delay, expressive speech disorder, dysarthria, dysphagia, gastroesophageal reflux disease, strabismus, ataxia, dysmorphisms including myopathic facies and overfolding of the superior helices, hockey-stick palmar creases, short anteverted nostrils, micropenis, and cryptorchidism. Brain MRI obtained at 7 years of age revealed small inferior posterior cerebellar lobes and hypoplasia of the posterior vermis with mild prominence of the ventricles and sulci (Figure 1B).

Proband 2 is a 5-year-old female of African American descent and has a de novo c.488G>A (p.Arg163Gln) missense change in *EBF3*. Her prenatal history is significant for decreased fetal movements, and she was born at full term at 40 weeks of gestation via induced vaginal delivery for oligohydramnios with a birth weight of 3.35 kg (25^{th}–50^{th} percentile). Her clinical features include congenital hypotonia, facial weakness, global developmental delay, expressive speech disorder, apraxia, dysarthria, dysphagia, strabismus, ataxia, perseverative social behaviors, dysmorphisms including triangular-shaped facies and overfolding of the superior helices, abnormal palmar creases, fifth-finger clinodactyly, and mild reduction in volume of the labia majora. She is reported to have marked insensitivity to pain such that she does not cry when she falls or receives vaccinations. Brain MRI obtained at 18 months of age revealed hypoplasia of the anterior and posterior vermis (Figure 1C).

Proband 3 is a 3-year-old female of English, Irish, German, and Polish descent and has a de novo c.488G>T (p.Arg163Leu) missense change in *EBF3*. Her prenatal history is significant for delivery at 39 weeks of gestation by caesarean section due to breech position and a birth weight of 2.7 kg (tenth percentile). Her clinical features include congenital hypotonia, facial weakness, global developmental delay, expressive speech disorder, dysphagia, motor stereotypies, and dysmorphisms including a triangular facies, small feet, and torticollis. She has no genitourinary abnormalities. At present, she speaks only one word, achieved ambulation late, and has a pincer grasp. She is reported to have marked insensitivity to pain such that she does not cry when she falls or receives vaccinations. Brain MRI obtained at 1 year of age was normal, and follow-up at 2 years of age was also normal (Figure 1D; a normal brain MRI axial image from a 23-month-old unaffected individual is included in Figure 1E for comparison).

All three probands presented here have neurodevelopmental disorders composed of intellectual disability, global developmental delay, ataxia, and motor incoordination (Figure 1 and Supplemental Note). Consistent neurological abnormalities in these probands include congenital hypotonia, facial weakness, dysphagia, and pronounced expressive speech disorder with dysarthria. Two probands also have decreased pain sensitivity. Brain anomalies are present in two of the three probands and include vermian hypoplasia with or without reduced cerebellar hemispheres. No other structural brain anomalies have been noted. Both probands with brain anomalies (1 and 2) have the de novo p.Arg163Gln variant. In contrast, proband 3 has the de novo p.Arg163Leu variant and lacks brain anomalies. Probands 1 and 2 have genitourinary defects, but proband 3 does not. A variety of dysmorphic features were also observed in the three probands (Figure 1 and Supplemental Note).

The recurrent de novo variant at the same nucleotide (c.488G>A [p.Arg163Gln]) is potentially due to the location of nucleotide 488 in a CpG-dinucleotide island. CpG-dinucleotide islands are mutational hotspots underlying over one-third of de novo missense variants associated with human diseases.[13,14] Given that paternal age was >40 years old for both probands with the p.Arg163Gln variant, other potential mechanisms are the selfish spermatogonial selection process proposed to underlie the association between advanced paternal age and neurodevelopmental disorders,[15] unrecognized side effects of the mutation resulting in recurrent de novo variants, or a selection bias for consistent neurodevelopmental phenotypes.

EBF3 is a downstream transcriptional target of aristaless-related homeobox (ARX) and is thought to be transcriptionally repressed by ARX. Gene-expression analysis performed on mouse *Arx*-mutant medial ganglionic eminence (MGE) showed that *Ebf3* had the highest increase in expression levels with the deletion of *Arx*. Furthermore, in vitro assays confirmed that Arx directly represses *Ebf3* expression, indicating that ARX and EBF3 share a strong molecular interaction in regulating γ-aminobutyric acid (GABA)ergic interneuron development and migration.[16,17]

Various mutations in *ARX* (MIM: 300382; HGNC: 18060) cause a diverse range of neurodevelopmental disorders ranging from structural CNS malformations and genitourinary abnormalities associated with premature truncation mutations (MIM: 300004 and 300215) to infantile spasms and epileptic encephalopathies associated with polyalanine repeats (MIM: 308350, 309510, and 300419) to isolated intellectual disability associated with missense mutations or *ARX* duplications (MIM: 300419).[16,18–24] Although the exact pathogenic nature of these *ARX* mutations remains to be fully elucidated, the types of mutations and CNVs suggest that haploinsufficient, gain-of-function, and dominant-negative mechanisms exist for *ARX*-related disorders.[18,21,23,25] Recent advances in sequencing technologies have revealed a growing number of putative *ARX* transcriptional targets identified by gene-expression analysis in *Arx* mouse models. At least three of the genes regulated by ARX, including *MAGEL2* (MIM: 605283 and 615547; HGNC: 6814),[26,27] *FOXP1* (MIM: 605515 and 613670; HGNC: 3823),[28,29] and *SOX8* (MIM: 605923 and 141750; HGNC: 11203),[30,31] are associated with neurodevelopmental disorders. These findings suggest that the transcriptional cascade mediated by ARX represents a pathway enriched with disease-associated genes in which mutations cause neurodevelopmental syndromes with

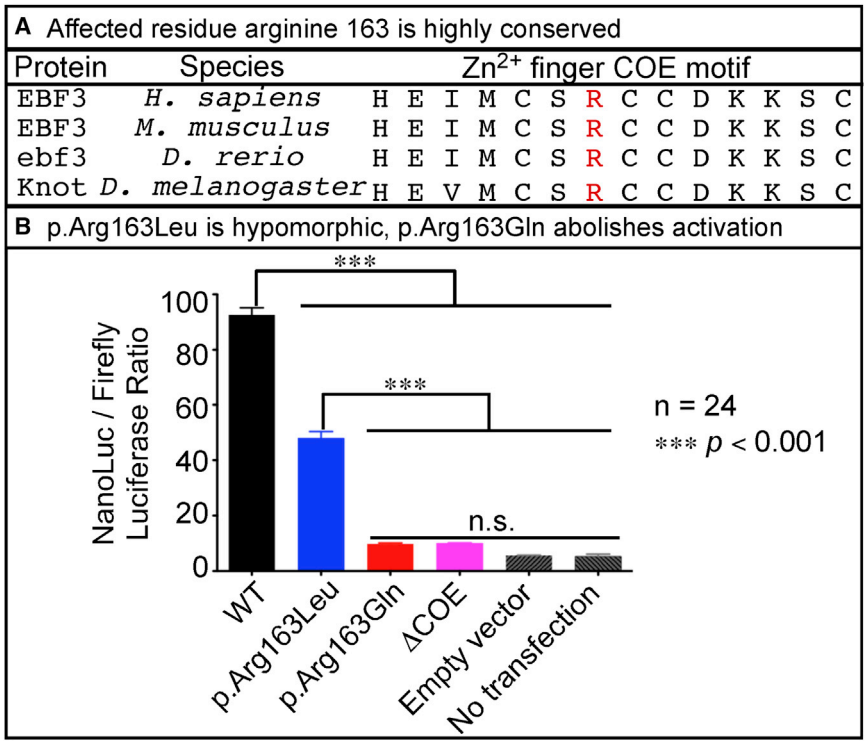

Figure 2. EBF3 p.Arg163Gln and p.Arg163Leu Impair Transcriptional Activation

(A) Affected residue Arg163 in the Zn^{2+} finger COE motif is highly conserved across vertebrates and invertebrates.

(B) Activation of reporter-gene expression in HEK293 cells was assessed as the ratio of NanoLuc to firefly luciferase according to the Promega NanoGlo Dual Reporter protocol and was measured on the TD 20/20 Luminometer. The cDNAs encoding WT EBF3 and the EBF3 p.Arg163Gln and p.Arg163Leu variants had a stop codon to ensure that the proteins were untagged to minimize off-target effects from a protein tag. The cDNAs were subcloned into the mammalian expression vector, pcDNA-DEST40. Two synthetic oligonucleotides containing the imperfect palindromic COE binding sequence were used to generate six concatamerized COE binding sites in the NanoLuc vector, pNL3.1. The pGL4.53 firefly luciferase vector was used as an internal transfection control. Additional experimental controls included EBF3 with deletion of the Zn^{2+} finger COE motif (denoted as ΔCOE). As transfection background controls, we either transfected only the pNL3.1 with six COE binding sites and pGL4.53 but no cDNA expression vectors (denoted as "empty vector") or did not transfect any vectors (denoted as "no transfection"). A 92-fold induction was observed with WT EBF3 (black). However, EBF3 p.Arg163Leu caused only a 45-fold induction (blue), indicating a partial loss of transcriptional activation. EBF3 p.Arg163Gln showed a very poor induction of transcription (red) similar in level to the transfection background (gray) and that of EBF3 ΔCOE (magenta) controls, indicating severe loss of activity. Data represent the mean ± SEM. n = 24 (six replicates per four separate transfections per experimental condition); ***$p < 0.001$ via one-way ANOVA with Tukey's post hoc analysis; n.s., no significant difference.

phenotypic features overlapping *ARX*-related disorders, such as *EBF3*.

Prior studies have shown that *Ebf3* haploinsufficiency in mice results in abnormal GABAergic interneuron migration and projection,[32] indicating that EBF3 is a critical regulator of inhibitory GABAergic neuronal development. EBF3 and other members of the COE family are also transiently expressed in Cajal-Retzius cells during corticogenesis, where these cells play an essential role in regulating laminar and areal specification.[33–37] Furthermore, extensive loss-of-function manipulations in well-conserved homologs of *EBF3* in worms (*unc-3*, also known as *CeO/E*), flies (*knot*, also known as *collier*), frogs (*Xcoe2*), and mice (*Ebf3*) have consistently been shown to impair survival and be deleterious to neuronal development, migration, and function[32,38–42]

The EBF3 Arg163 residue affected in all three probands is a highly conserved arginine across vertebrate and invertebrate species and is located in the Zn^{2+} finger COE motif ($H\text{-}X_3C\text{-}X_2\text{-}C\text{-}X_5\text{-}C$) present in the amino-terminal DNA-binding domain (Figure 2A). A prior mutational study of the paralogous EBF1 showed that disrupting highly conserved cysteine and histidine residues in the 14-aa COE motif abolishes DNA-binding activity by destabilizing the conformation of the Zn^{2+} finger COE motif.[43] In the same study, EBF1 p.Arg163Ala also affected DNA binding.[43] To assess the functional consequences of p.Arg163Gln and p.Arg163Leu on EBF3 activation of gene expression, we performed a luciferase activity assay by utilizing previously identified COE transcription factor binding sites.[44,45] To generate the *EBF3* variants, we utilized the human full-length cDNA clone for the most abundant splicing isoform of *EBF3* (full-length ORF [GenBank: HQ258299] and mRNA [GenBank: BC130479.1]). Site-directed mutagenesis was performed for *EBF3* in the pENTR223 Gateway compatible donor vector via either the Agilent QuikChange Lightning or the NEB Q5 site-directed mutagenesis protocol.

We compared the transcriptional activity of the EBF3 variants to that of two controls: wild-type (WT) EBF3 and EBF3 with deletion of the Zn^{2+} finger COE motif (ΔCOE). HEK293 cells were co-transfected with each individual *EBF3* cDNA expression construct in combination with nanoluciferase (NanoLuc) and firefly luciferase vectors. Activation of reporter-gene expression in vitro was assessed as the ratio of NanoLuc to firefly luciferase. A 92-fold induction was observed with WT EBF3. However, EBF3 p.Arg163Leu had only a 45-fold induction, suggesting that the variant is a hypomorphic alteration. EBF3 p.Arg163Gln showed a very poor induction similar in level to the transfection background and that of EBF3 ΔCOE controls, indicating that it is a severe loss-of-function variant (Figure 2B).

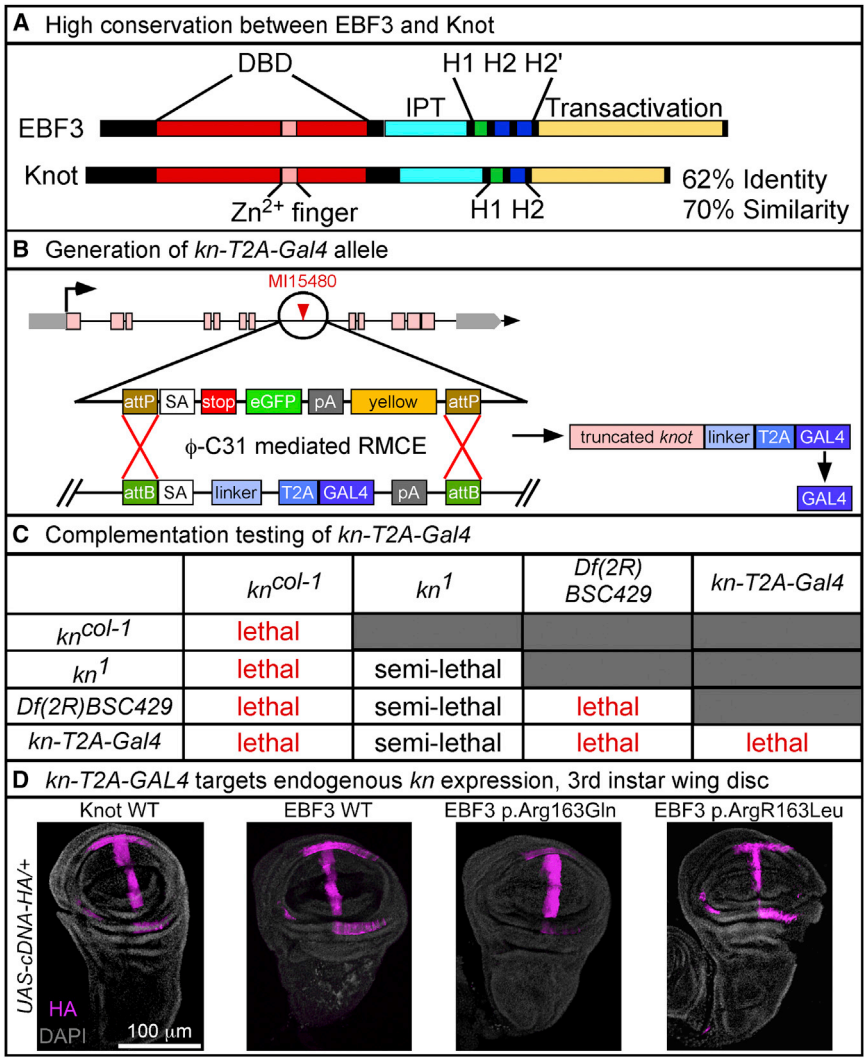

Figure 3. Generation and Characterization of the Fly *kn*-T2A-GAL4 Allele

(A) High conservation of protein structure and amino acid sequence between human EBF3 and fly Knot with 62% identity and 70% similarity. Conserved domains include the DNA-binding domain (DBD, red), Zn^{2+} finger COE motif (pink), Ig-like/plexins/transcription factors (IPT) domain (cyan), helix-loop-helix dimerization motif with α helices H1 (green) and H2 or H2′ (blue), and C-terminal transactivation domain (yellow).

(B) Conversion of the MI15480 line with a MiMIC transposable-element insertion in the fourth coding intron of *knot* via ϕC31-mediated RMCE for generation of the *kn-T2A-GAL4* allele, which expresses GAL4 transactivator in the pattern of *kn*. This allele also creates a loss-of-function allele of *knot* by prematurely truncating the transcript by a ribosomal skipping signal (T2A) and a premature polyadenylation signal (pA).

(C) Complementation testing shows that *kn-T2A-GAL4* with both the amorphic kn^{col-1} and genomic deficiency *Df(2R) BSC429*, encompassing the entire *kn* locus, fails to complement the lethality. Complementation with hypomorphic kn^{1} is semi-lethal with <10% viability.

(D) For expression analysis, *yw/y; kn-T2A-GAL4/CyO, Kr-GAL4, UAS-GFP* males were crossed with *yw; UAS-cDNA/TM3 Sb, Kr-GAL4, UAS-GFP* virgin females, and double heterozygotes were selected by loss of GFP expression. Images were acquired on a Leica Sp8 laser-scanning confocal microscope. The same settings for laser power and detector gain were used for all genotypes. Images were acquired as a z stack with a z-step of 1 μm and line average of 4 at 400 Hz with a 25× water objective at 1024 × 1024 pixel resolution. Maximum intensity projections were created from the stack in ImageJ. Immunolabeling revealed that *kn-T2A-GAL4* recapitulates the endogenous *knot* expression pattern in third instar wing disc, as shown with the HA-tagged *UAS* fly lines for WT Knot, WT EBF3, and the EBF3 p.Arg163Gln and p.Arg163Leu variants. Images show HA (magenta) and DAPI (gray). The scale bar represents 100 μm.

To decipher the functional significance of the observed de novo variants affecting residue Arg163, we turned to a recently proposed method to test their pathogenicity in vivo in flies.[46] *EBF3* is one of four COE homologs in mammals, but *Drosophila melanogaster* has only one COE transcription factor, *knot*, also known as *collier* (gene symbol: *kn* [FlyBase: FBgn0001319]), which has 62% identity with and 70% similarity to *EBF3* (Figure 3A). Prior studies in the fly have shown that loss of *knot* function is detrimental to nervous system development and that homozygous-null alleles of *knot* are embryonically lethal.[39,40,47] We utilized rescue of the homozygous embryonically lethal phenotype and the availability of sophisticated genetic tools to assess the human *EBF3* variants by taking advantage of a Minos-mediated integration cassette (MiMIC) transposon inserted in the fourth coding intron of *knot* (Figure 3B).[48,49] Utilizing recombinase-mediated cassette exchange (RMCE), we created a novel *knot* allele that truncates the *knot* transcript and expresses the yeast transactivator gene, *GAL4*, under the control of the endogenous regulatory elements of *knot* (Figure 3B).[50,51] Heterozygous *kn-T2A-GAL4* flies are viable and do not show any obvious phenotype. Complementation testing showed that the *kn-T2A-GAL4* is a severe loss-of-function or null allele causing homozygous embryonic lethality. *kn-T2A-GAL4* also fails to complement the lethality of the previously well-characterized amorphic kn^{col-1} allele,[40] the hypomorphic kn^{1} allele,[47] and a molecularly defined deficiency allele, *Df(2R)BSC429*, which includes the *kn* locus[52] (Figure 3C), confirming the specificity of the *kn-T2A-GAL4* mutation.

To assess the functional significance of the EBF3 p.Arg163Gln and p.Arg163Leu variants in flies, we generated several transgenic fly alleles by utilizing the pUASg-HA-attB vector[53] to express the human WT *EBF3* and variant cDNAs with a C-terminal hemagglutinin (HA) tag

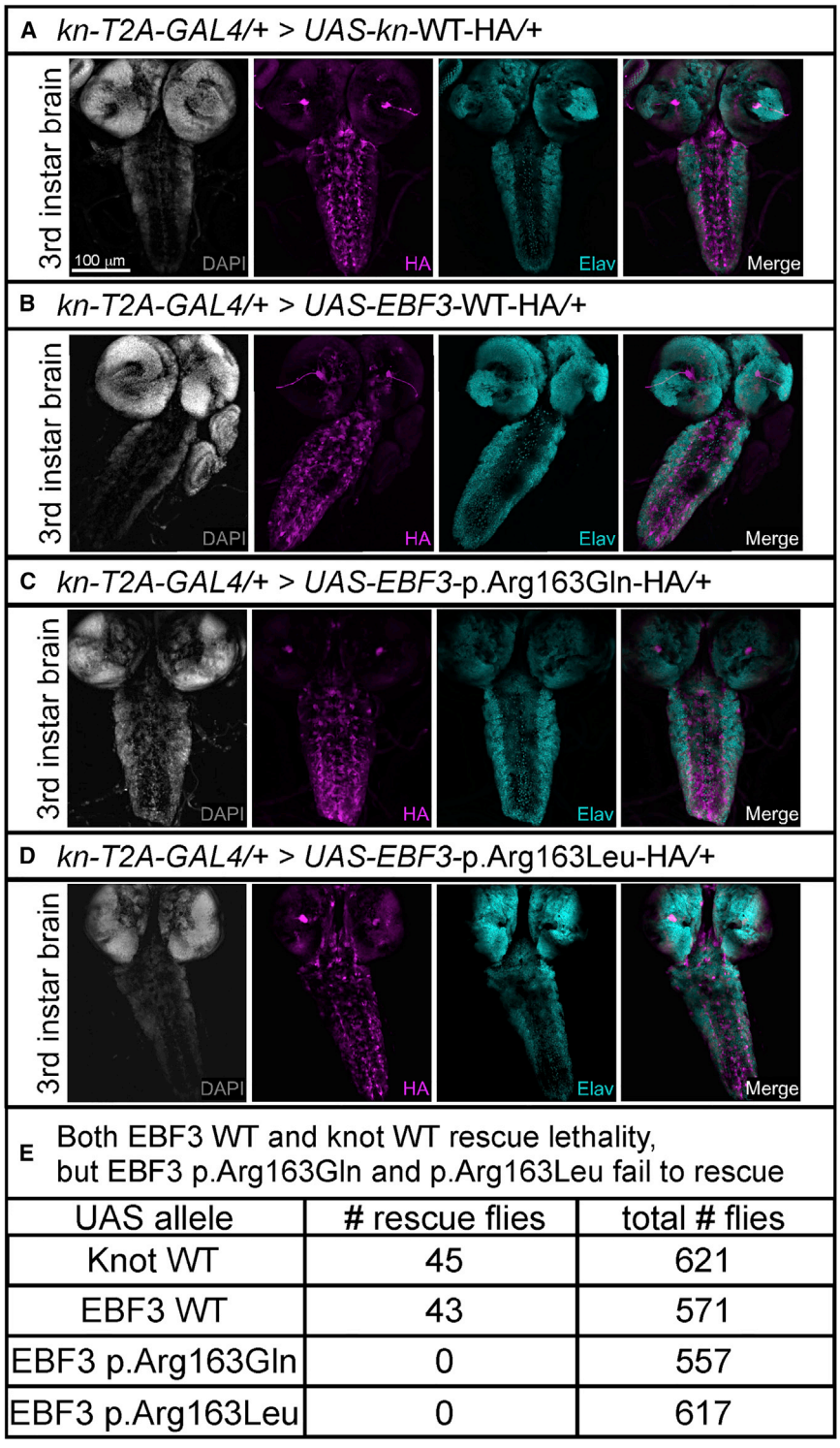

E Both EBF3 WT and knot WT rescue lethality, but EBF3 p.Arg163Gln and p.Arg163Leu fail to rescue

UAS allele	# rescue flies	total # flies
Knot WT	45	621
EBF3 WT	43	571
EBF3 p.Arg163Gln	0	557
EBF3 p.Arg163Leu	0	617

Figure 4. WT *EBF3* and *knot* Rescue Lethality, but EBF3 p.Arg163Gln and p.Arg163Leu Fail to Rescue Lethality in Flies

(A–D) For expression analysis of third instar brain and ventral nerve cord, *yw/y; kn-T2A-GAL4/CyO, Kr-GAL4, UAS-GFP* males were crossed with *yw; UAS-cDNA/TM3 Sb, Kr-GAL4, UAS-GFP* virgin females, and double heterozygotes were selected by loss of GFP expression in the wandering third instar larval stage. Images were acquired on a Leica Sp8 laser-scanning confocal microscope. The same settings for laser power and detector gain were used for all genotypes. Third instar larval brain images were acquired as a z stack with a z-step of 1.51 μm and line average of 4 at 400 Hz with a 20× objective at 1024 × 1024 pixel resolution. Maximum intensity projections were created from the stack in ImageJ. Immunolabeling revealed that *kn-T2A-GAL4* drives expression of HA-tagged *UAS* fly lines for WT Knot (A), WT EBF3 (B), EBF3 p.Arg163Gln (C), and EBF3 p.Arg163Leu (D) in the third instar brain and ventral nerve cord (pan-neuronal marker Elav in cyan; nuclei labeled with DAPI in gray). The scale bar represents 100 μm.

(E) Fly in vivo rescue analysis using the UAS-GAL4 system. For generating the rescue flies, w^{1118}*/y; Df(2R)BSC429/Sp; UAS-cDNA-WT-HA/+* males were crossed with *yw; kn-T2A-GAL4/SM6a* virgin females to produce rescue animals with Knot or EBF3 produced solely from the UAS allele under the control of the *kn-T2A-GAL4* driver. The genotypes of the rescued flies are *yw/y; Df(2R)BSC429/kn-T2A-GAL4; UAS-cDNA-HA/+* males and w^{1118}*/yw; ; Df(2R)BSC429/kn-T2A-GAL4; UAS-cDNA-HA/+* females. For each *UAS-cDNA* line, >550 adult flies were scored; data represent the number of observed rescue flies and the total number of flies scored. *UAS* fly lines expressing WT Knot or WT EBF3 rescued embryonic lethality in viable adults. *UAS* fly lines expressing EBF3 variant p.Arg163Gln or p.Arg163Leu completely failed to rescue the lethality such that no rescue animals were observed as adults or pupae.

under the control of upstream activating system (UAS) elements. As an internal control, we assessed rescue with the WT *knot* fly cDNA with a C-terminal HA tag under the control of UAS. In conjunction with the *kn-T2A-GAL4* allele, the UAS-GAL4 system allowed us to express the human *EBF3* and fly *knot* cDNAs in the same endogenous spatiotemporal pattern as *knot*. We determined that *kn-T2A-GAL4* recapitulates the previously characterized endogenous expression pattern of Knot in the wing imaginal disc of third instar larvae for the UAS lines encoding WT Knot, WT EBF3, and the EBF3 p.Arg163Gln and p.Arg163Leu variants when probed with anti-HA (magenta) (Figure 3D).[47]

We also determined that *kn-T2A-GAL4* drives expression of WT Knot, WT EBF3, and the EBF3 p.Arg163Gln and p.Arg163Leu variants when probed with anti-HA (magenta) in a similar subset of neurons labeled with the pan-neuronal marker Elav (cyan) in the third instar larval brain and ventral nerve cord (Figures 4A–4D). These data

suggest that the GAL4 produced by the fusion transcript is expressed in the proper spatial and temporal expression pattern.

To determine the in vivo functional consequences of the EBF3 p.Arg163Gln and p.Arg163Leu variants, we utilized the UAS-GAL4 system with the *kn-T2A-GAL4* allele to assess whether WT Knot, WT EBF3, and EBF3 p.Arg163Gln and p.Arg163Leu are capable of rescuing the embryonic lethality observed with complete loss of endogenous Knot. We scored >550 adult flies per cDNA variant and found that both WT EBF3 and WT Knot rescued the embryonic lethality at near Mendelian expectations but that both the EBF3 p.Arg163Gln and p.Arg163Leu variants failed to rescue the lethality, and no adults or pupae were observed (Figure 4E).

Together, the in vitro luciferase reporter-gene activation assay and in vivo fly functional assessment demonstrate that our probands' de novo *EBF3* variants result in a loss of EBF3 function in activating transcription, which is consistent with prior in vitro findings showing that altering the charged Arg163 to neutral alanine abolishes DNA binding.[43] Pathogenic mechanisms for these variants could potentially be gain of function, haploinsufficiency loss of function, and dominant negative. A gain-of-function mechanism is less likely given the luciferase data and the near complete loss of activation of reporter-gene expression. The normal development of heterozygous kn^{col-1} flies and the subtle morphological phenotypes displayed in mice with *Ebf3* haploinsufficiency suggest that haploinsufficiency might not solely contribute to the observed phenotypes in our probands. However, the prior findings in fly and mouse models are limited in the assessment of the in vivo consequences of *knot* or *Ebf3* haploinsufficiency to neural network activity and behaviors, and we therefore cannot exclude haploinsufficiency on the basis of these results from prior animal models.

Deletions of at least part of the *EBF3* locus have been observed in 59 of 21,770 samples in DECIPHER; they range in size from 120 kb to 14.49 Mb and are associated with syndromic neurodevelopmental features including cerebellar vermian hypoplasia, behavioral abnormalities, motor stereotypies, intellectual disability, delayed speech and language, motor delay, seizures, and genitourinary abnormalities, which were observed in our three probands.[54] The majority of these deletion CNVs were reported as de novo in DECIPHER, but some were also inherited from a reportedly unaffected parent, suggesting that the parent might have somatic mosaicism for the CNV or genetic modifiers of phenotypic severity. The smallest deletion encompassing the entire *EBF3* locus was 656 kb and only included two genes in addition to *EBF3*.

In contrast, the Database of Genomic Variants (DGV) reports no CNVs with deletion of the entire *EBF3* locus in 54,946 samples from the general population.[55] However, the DGV does report two individuals with deletion CNVs (1.25 and 1.34 Mb) containing a breakpoint within the *EBF3* locus. Given that the full phenotypic range of *EBF3* loss of function has not been elucidated, it remains to be determined whether these reportedly unaffected individuals carrying *EBF3* deletion CNVs might represent the milder presentation of *EBF3* loss of function or are unaffected carriers. Relative to those in reportedly unaffected individuals in the general population, the enrichment of *EBF3* deletion CNVs reported in affected individuals with a range of neurodevelopmental phenotypes, together with the phenotypic overlap between our probands and de novo loss-of-function variants in *EBF3*, suggests that haploinsufficiency of *EBF3* is potentially pathogenic. Given that EBF3 transcription factors function as homodimers that bind to each other via their basic helix-loop-helix domain, another potential mechanism for the loss of function observed with variants p.Arg163Gln and p.Arg163Leu could be that they correspond to dominant-negative mutations that poison the function of the WT protein. The autosomal-dominant mode of inheritance of these variants is therefore most likely due to EBF3 loss of function via either a dominant-negative or haploinsufficient effect.

Interestingly, *EBF3* is a well-characterized transcriptional target of *ARX*, and loss of ARX repression of *EBF3* causes disrupted inhibitory GABAergic neuronal migration in *Arx*-deletion mouse models. Our findings suggest that *EBF3* loss of function might mediate a subset of features seen in *ARX*-related disorders associated with *ARX* gain of function, specifically with regard to the shared features of intellectual disability, abnormal genitalia, and structural CNS anomalies. Additionally, the phenotypes of the three probands are clearly similar and consistent with the functional results for the EBF3 p.Arg163Gln and p.Arg163Leu variants. We show that EBF3 p.Arg163Gln is a severe loss-of-function variant and that p.Arg163Leu is a partial loss-of-function variant. Determining possible genotype-phenotype correlations related to residual activity of the variant protein is limited by the small sample size. However, it is interesting that probands 1 and 2 (who have the p.Arg163Gln variant and minimal transcriptional activity) have structural anomalies of the cerebellum, whereas proband 3 (who has the p.Arg163Leu variant and partial transcriptional activity) has no structural brain or genitourinary abnormalities. We also note that Harms et al.[56] (in this issue of *The Journal*) identify *EBF3* mutations in individuals with similar neurological phenotypes. A larger sample size and longitudinal monitoring of neurodevelopment would be beneficial to determining the genotype-phenotype correlations between the *EBF3* variants identified in the two studies. Our findings further suggest that *ARX* target genes might represent an enriched population of disease-associated genes for neurodevelopmental disorders given the diversity and heterogeneity of *ARX*-related disorders.

Accession Numbers

The accession numbers for the c.488G>A (p.Arg163Gln) and c.488G>T (p.Arg163Leu) sequences reported in this paper are ClinVar: SCV000328550 and SCV000328551, respectively.

Supplemental Data

Supplemental Data include a Supplemental Note and six tables and can be found with this article online at http://dx.doi.org/10.1016/j.ajhg.2016.11.018.

Consortia

Members of the Undiagnosed Diseases Network (UDN) include David R. Adams, Christopher J. Adams, Mercedes E. Alejandro, Patrick Allard, Euan A. Ashley, Carlos A. Bacino, Ashok Balasubramanyam, Hayk Barseghyan, Alan H. Beggs, Hugo J. Bellen, Jonathan A. Bernstein, David P. Bick, Camille L. Birch, Braden E. Boone, Lauren C. Briere, Donna M. Brown, Matthew Brush, Lindsay C. Burrage, Katherine R. Chao, Gary D. Clark, Joy D. Cogan, Cynthia M. Cooper, William J. Craigen, Mariska Davids, Jyoti G. Dayal, Esteban C. Dell'Angelica, Shweta U. Dhar, Katrina M. Dipple, Laurel A. Donnell-Fink, Naghmeh Dorrani, Dan C. Dorset, David D. Draper, Annika M. Dries, David J. Eckstein, Lisa T. Emrick, Christine M. Eng, Cecilia Esteves, Tyra Estwick, Paul G. Fisher, Trevor S. Frisby, Kate Frost, William A. Gahl, Valerie Gartner, Rena A. Godfrey, Mitchell Goheen, Gretchen A. Golas, David B. Goldstein, Mary "Gracie" G. Gordon, Sarah E. Gould, Jean-Philippe F. Gourdine, Brett H. Graham, Catherine A. Groden, Andrea L. Gropman, Mary E. Hackbarth, Melissa Haendel, Rizwan Hamid, Neil A. Hanchard, Lori H. Handley, Isabel Hardee, Matthew R. Herzog, Ingrid A. Holm, Ellen M. Howerton, Howard J. Jacob, Mahim Jain, Yonghui Jiang, Jean M. Johnston, Angela L. Jones, Alanna E. Koehler, David M. Koeller, Isaac S. Kohane, Jennefer N. Kohler, Donna M. Krasnewich, Elizabeth L. Krieg, Joel B. Krier, Jennifer E. Kyle, Seema R. Lalani, Lea Latham, Yvonne L. Latour, C. Christopher Lau, Jozef Lazar, Brendan H. Lee, Hane Lee, Paul R. Lee, Shawn E. Levy, Denise J. Levy, Richard A. Lewis, Adam P. Liebendorder, Sharyn A. Lincoln, Carson R. Loomis, Joseph Loscalzo, Richard L. Maas, Ellen F. Macnamara, Calum A. MacRae, Valerie V. Maduro, May Christine V. Malicdan, Laura A. Mamounas, Teri A. Manolio, Thomas C. Markello, Azamian S. Mashid, Paul Mazur, Alexandra J. McCarty, Allyn McConkie-Rosell, Alexa T. McCray, Thomas O. Metz, Matthew Might, Paolo M. Moretti, John J. Mulvihill, Jennifer L. Murphy, Donna M. Muzny, Michele E. Nehrebecky, Stan F. Nelson, J. Scott Newberry, John H. Newman, Sarah K. Nicholas, Donna Novacic, Jordan S. Orange, J. Carl Pallais, Christina G.S. Palmer, Jeanette C. Papp, Loren D.M. Pena, John A. Phillips III, Jennifer E. Posey, John H. Postlethwait, Lorraine Potocki, Barbara N. Pusey, Rachel B. Ramoni, Lance H. Rodan, Sarah Sadozai, Katherine E. Schaffer, Kelly Schoch, Molly C. Schroeder, Daryl A. Scott, Prashant Sharma, Vandana Shashi, Edwin K. Silverman, Janet S. Sinsheimer, Ariane G. Soldatos, Rebecca C. Spillmann, Kimberly Splinter, Joan M. Stoler, Nicholas Stong, Kimberly A. Strong, Jennifer A. Sullivan, David A. Sweetser, Sara P. Thomas, Cynthia J. Tift, Nathanial J. Tolman, Camilo Toro, Alyssa A. Tran, Zaheer M. Valivullah, Eric Vilain, Daryl M. Waggott, Colleen E. Wahl, Nicole M. Walley, Chris A. Walsh, Michael F. Wangler, Mike Warburton, Patricia A. Ward, Katrina M. Waters, Bobbie-Jo M. Webb-Robertson, Alec A. Weech, Monte Westerfield, Matt T. Wheeler, Anastasia L. Wise, Lynne A. Worthe, Elizabeth A. Worthey, Shinya Yamamoto, Yaping Yang, Guoyun Yu, and Patricia A. Zornio.

Acknowledgments

We thank the families and clinical staff at the Undiagnosed Diseases Program (UDP), Baylor College of Medicine (BCM), and New York University for participating in this study. This work was supported in part by NIH grants U54NS093793, R24OD022005, and R01GM067858 to H.J.B, by the Intramural Research Program of the National Human Genome Research Institute, and by the Common Fund of the NIH Office of the Director. H.J.B. is an investigator of the Howard Hughes Medical Institute (HHMI). F.X. and J.A.R. are supported by NIH grant U01HG007709. The Department of Molecular and Human Genetics at BCM derives revenue from the clinical exome sequencing offered at Baylor Genetics. We are thankful for the technical assistance provided by Y. Huang (NIH UDP Translational Laboratory) for Sanger sequencing; A. Weech (NIH UDP Translational Laboratory) for input on protein modeling; H. Pan (HHMI, BCM) for fly embryo injections; S. Nagarkar-Jaiswal, P. Lee, Y. He, J. Li, Z. Wang, Q. Gao, and L. Wang (BCM) for creating the 15,000 MiMIC insertion stocks; and W. Lin (BCM) for T2A-GAL4 conversion. We thank the Bloomington Drosophila Stock Center, Drosophila Genomics and Genetic Resources, and FlyORF for numerous stocks and the Developmental Studies Hybridoma Bank for antibodies. This study made use of data generated by the DECIPHER community. A full list of centers that contributed to the generation of the data is available at http://decipher.sanger.ac.uk and via email at decipher@sanger.ac.uk. Funding for the project was provided by the Wellcome Trust.

Received: September 2, 2016
Accepted: November 21, 2016
Published: December 22, 2016

Web Resources

ClinVar, https://www.ncbi.nlm.nih.gov/clinvar/
Database of Genomic Variation (DGV), http://dgv.tcag.ca/dgv/app/home/
DECIPHER, http://decipher.sanger.ac.uk/
ENSEMBL Variant Effect Predictor, http://useast.ensembl.org/info/docs/tools/vep/index.html
Exome Aggregation Consortium (ExAC) Browser, http://exac.broadinstitute.org/
FlyBase, http://flybase.org/
GenBank, https://www.ncbi.nlm.nih.gov/genbank/
MutationTaster, http://www.mutationtaster.org
OMIM, http://www.omim.org/
PolyPhen-2, http://genetics.bwh.harvard.edu/pph2/

References

1. Alwan, A., and Modell, B. (2003). Recommendations for introducing genetics services in developing countries. Nat. Rev. Genet. *4*, 61–68.
2. American Psychiatric Association, ed. (2013). Diagnostic and statistical manual of mental disorders, Fifth Edition (American Psychiatric Association Publishing).
3. Boivin, M.J., Kakooza, A.M., Warf, B.C., Davidson, L.L., and Grigorenko, E.L. (2015). Reducing neurodevelopmental disorders and disability through research and interventions. Nature *527*, S155–S160.
4. Yang, Y., Muzny, D.M., Reid, J.G., Bainbridge, M.N., Willis, A., Ward, P.A., Braxton, A., Beuten, J., Xia, F., Niu, Z., et al. (2013). Clinical whole-exome sequencing for the diagnosis of mendelian disorders. N. Engl. J. Med. *369*, 1502–1511.
5. Zhu, X., Petrovski, S., Xie, P., Ruzzo, E.K., Lu, Y.F., McSweeney, K.M., Ben-Zeev, B., Nissenkorn, A., Anikster, Y., Oz-Levi, D.,

et al. (2015). Whole-exome sequencing in undiagnosed genetic diseases: interpreting 119 trios. Genet. Med. *17*, 774–781.
6. de Ligt, J., Willemsen, M.H., van Bon, B.W., Kleefstra, T., Yntema, H.G., Kroes, T., Vulto-van Silfhout, A.T., Koolen, D.A., de Vries, P., Gilissen, C., et al. (2012). Diagnostic exome sequencing in persons with severe intellectual disability. N. Engl. J. Med. *367*, 1921–1929.
7. Neale, B.M., Kou, Y., Liu, L., Ma'ayan, A., Samocha, K.E., Sabo, A., Lin, C.F., Stevens, C., Wang, L.S., Makarov, V., et al. (2012). Patterns and rates of exonic de novo mutations in autism spectrum disorders. Nature *485*, 242–245.
8. Bainbridge, M.N., Hu, H., Muzny, D.M., Musante, L., Lupski, J.R., Graham, B.H., Chen, W., Gripp, K.W., Jenny, K., Wienker, T.F., et al. (2013). De novo truncating mutations in ASXL3 are associated with a novel clinical phenotype with similarities to Bohring-Opitz syndrome. Genome Med. *5*, 11.
9. Allen, A.S., Berkovic, S.F., Cossette, P., Delanty, N., Dlugos, D., Eichler, E.E., Epstein, M.P., Glauser, T., Goldstein, D.B., Han, Y., et al.; Epi4K Consortium; and Epilepsy Phenome/Genome Project (2013). De novo mutations in epileptic encephalopathies. Nature *501*, 217–221.
10. Petrovski, S., Wang, Q., Heinzen, E.L., Allen, A.S., and Goldstein, D.B. (2013). Genic intolerance to functional variation and the interpretation of personal genomes. PLoS Genet. *9*, e1003709.
11. Samocha, K.E., Robinson, E.B., Sanders, S.J., Stevens, C., Sabo, A., McGrath, L.M., Kosmicki, J.A., Rehnström, K., Mallick, S., Kirby, A., et al. (2014). A framework for the interpretation of de novo mutation in human disease. Nat. Genet. *46*, 944–950.
12. Lek, M., Karczewski, K.J., Minikel, E.V., Samocha, K.E., Banks, E., Fennell, T., O'Donnell-Luria, A.H., Ware, J.S., Hill, A.J., Cummings, B.B., et al.; Exome Aggregation Consortium (2016). Analysis of protein-coding genetic variation in 60,706 humans. Nature *536*, 285–291.
13. Magewu, A.N., and Jones, P.A. (1994). Ubiquitous and tenacious methylation of the CpG site in codon 248 of the p53 gene may explain its frequent appearance as a mutational hot spot in human cancer. Mol. Cell. Biol. *14*, 4225–4232.
14. Mancini, D., Singh, S., Ainsworth, P., and Rodenhiser, D. (1997). Constitutively methylated CpG dinucleotides as mutation hot spots in the retinoblastoma gene (RB1). Am. J. Hum. Genet. *61*, 80–87.
15. Goriely, A., McGrath, J.J., Hultman, C.M., Wilkie, A.O., and Malaspina, D. (2013). "Selfish spermatogonial selection": a novel mechanism for the association between advanced paternal age and neurodevelopmental disorders. Am. J. Psychiatry *170*, 599–608.
16. Colasante, G., Sessa, A., Crispi, S., Calogero, R., Mansouri, A., Collombat, P., and Broccoli, V. (2009). Arx acts as a regional key selector gene in the ventral telencephalon mainly through its transcriptional repression activity. Dev. Biol. *334*, 59–71.
17. Fulp, C.T., Cho, G., Marsh, E.D., Nasrallah, I.M., Labosky, P.A., and Golden, J.A. (2008). Identification of Arx transcriptional targets in the developing basal forebrain. Hum. Mol. Genet. *17*, 3740–3760.
18. Strømme, P., Mangelsdorf, M.E., Shaw, M.A., Lower, K.M., Lewis, S.M., Bruyere, H., Lütcherath, V., Gedeon, A.K., Wallace, R.H., Scheffer, I.E., et al. (2002). Mutations in the human ortholog of Aristaless cause X-linked mental retardation and epilepsy. Nat. Genet. *30*, 441–445.
19. Bienvenu, T., Poirier, K., Friocourt, G., Bahi, N., Beaumont, D., Fauchereau, F., Ben Jeema, L., Zemni, R., Vinet, M.C., Francis, F., et al. (2002). ARX, a novel Prd-class-homeobox gene highly expressed in the telencephalon, is mutated in X-linked mental retardation. Hum. Mol. Genet. *11*, 981–991.
20. Kato, M., Das, S., Petras, K., Kitamura, K., Morohashi, K., Abuelo, D.N., Barr, M., Bonneau, D., Brady, A.F., Carpenter, N.J., et al. (2004). Mutations of ARX are associated with striking pleiotropy and consistent genotype-phenotype correlation. Hum. Mutat. *23*, 147–159.
21. Kato, M., Saitoh, S., Kamei, A., Shiraishi, H., Ueda, Y., Akasaka, M., Tohyama, J., Akasaka, N., and Hayasaka, K. (2007). A longer polyalanine expansion mutation in the ARX gene causes early infantile epileptic encephalopathy with suppression-burst pattern (Ohtahara syndrome). Am. J. Hum. Genet. *81*, 361–366.
22. Kitamura, K., Yanazawa, M., Sugiyama, N., Miura, H., Iizuka-Kogo, A., Kusaka, M., Omichi, K., Suzuki, R., Kato-Fukui, Y., Kamiirisa, K., et al. (2002). Mutation of ARX causes abnormal development of forebrain and testes in mice and X-linked lissencephaly with abnormal genitalia in humans. Nat. Genet. *32*, 359–369.
23. Ishibashi, M., Manning, E., Shoubridge, C., Krecsmarik, M., Hawkins, T.A., Giacomotto, J., Zhao, T., Mueller, T., Bader, P.I., Cheung, S.W., et al. (2015). Copy number variants in patients with intellectual disability affect the regulation of ARX transcription factor gene. Hum. Genet. *134*, 1163–1182.
24. Turner, G., Partington, M., Kerr, B., Mangelsdorf, M., and Gecz, J. (2002). Variable expression of mental retardation, autism, seizures, and dystonic hand movements in two families with an identical ARX gene mutation. Am. J. Med. Genet. *112*, 405–411.
25. Okazaki, S., Ohsawa, M., Kuki, I., Kawawaki, H., Koriyama, T., Ri, S., Ichiba, H., Hai, E., Inoue, T., Nakamura, H., et al. (2008). Aristaless-related homeobox gene disruption leads to abnormal distribution of GABAergic interneurons in human neocortex: evidence based on a case of X-linked lissencephaly with abnormal genitalia (XLAG). Acta Neuropathol. *116*, 453–462.
26. Schaaf, C.P., Gonzalez-Garay, M.L., Xia, F., Potocki, L., Gripp, K.W., Zhang, B., Peters, B.A., McElwain, M.A., Drmanac, R., Beaudet, A.L., et al. (2013). Truncating mutations of MAGEL2 cause Prader-Willi phenotypes and autism. Nat. Genet. *45*, 1405–1408.
27. Fountain, M.D., Aten, E., Cho, M.T., Juusola, J., Walkiewicz, M.A., Ray, J.W., Xia, F., Yang, Y., Graham, B.H., Bacino, C.A., et al. (2016). The phenotypic spectrum of Schaaf-Yang syndrome: 18 new affected individuals from 14 families. Genet. Med.
28. Le Fevre, A.K., Taylor, S., Malek, N.H., Horn, D., Carr, C.W., Abdul-Rahman, O.A., O'Donnell, S., Burgess, T., Shaw, M., Gecz, J., et al. (2013). FOXP1 mutations cause intellectual disability and a recognizable phenotype. Am. J. Med. Genet. A. *161A*, 3166–3175.
29. Horn, D., Kapeller, J., Rivera-Brugués, N., Moog, U., Lorenz-Depiereux, B., Eck, S., Hempel, M., Wagenstaller, J., Gawthrope, A., Monaco, A.P., et al. (2010). Identification of FOXP1 deletions in three unrelated patients with mental retardation and significant speech and language deficits. Hum. Mutat. *31*, E1851–E1860.
30. Pfeifer, D., Poulat, F., Holinski-Feder, E., Kooy, F., and Scherer, G. (2000). The SOX8 gene is located within 700 kb of the tip of

chromosome 16p and is deleted in a patient with ATR-16 syndrome. Genomics *63*, 108–116.
31. Harteveld, C.L., Kriek, M., Bijlsma, E.K., Erjavec, Z., Balak, D., Phylipsen, M., Voskamp, A., di Capua, E., White, S.J., and Giordano, P.C. (2007). Refinement of the genetic cause of ATR-16. Hum. Genet. *122*, 283–292.
32. Wang, S.S., Lewcock, J.W., Feinstein, P., Mombaerts, P., and Reed, R.R. (2004). Genetic disruptions of O/E2 and O/E3 genes reveal involvement in olfactory receptor neuron projection. Development *131*, 1377–1388.
33. Chiara, F., Badaloni, A., Croci, L., Yeh, M.L., Cariboni, A., Hoerder-Suabedissen, A., Consalez, G.G., Eickholt, B., Shimogori, T., Parnavelas, J.G., and Rakić, S. (2012). Early B-cell factors 2 and 3 (EBF2/3) regulate early migration of Cajal-Retzius cells from the cortical hem. Dev. Biol. *365*, 277–289.
34. Cooper, J.A. (2008). A mechanism for inside-out lamination in the neocortex. Trends Neurosci. *31*, 113–119.
35. Garel, S., Marín, F., Mattéi, M.G., Vesque, C., Vincent, A., and Charnay, P. (1997). Family of Ebf/Olf-1-related genes potentially involved in neuronal differentiation and regional specification in the central nervous system. Dev. Dyn. *210*, 191–205.
36. Yamazaki, H., Sekiguchi, M., Takamatsu, M., Tanabe, Y., and Nakanishi, S. (2004). Distinct ontogenic and regional expressions of newly identified Cajal-Retzius cell-specific genes during neocorticogenesis. Proc. Natl. Acad. Sci. USA *101*, 14509–14514.
37. Chowdhury, T.G., Jimenez, J.C., Bomar, J.M., Cruz-Martin, A., Cantle, J.P., and Portera-Cailliau, C. (2010). Fate of cajal-retzius neurons in the postnatal mouse neocortex. Front. Neuroanat. *4*, 10.
38. Liberg, D., Sigvardsson, M., and Akerblad, P. (2002). The EBF/Olf/Collier family of transcription factors: regulators of differentiation in cells originating from all three embryonal germ layers. Mol. Cell. Biol. *22*, 8389–8397.
39. Crozatier, M., Valle, D., Dubois, L., Ibnsouda, S., and Vincent, A. (1996). Collier, a novel regulator of Drosophila head development, is expressed in a single mitotic domain. Curr. Biol. *6*, 707–718.
40. Crozatier, M., Valle, D., Dubois, L., Ibnsouda, S., and Vincent, A. (1999). Head versus trunk patterning in the Drosophila embryo; collier requirement for formation of the intercalary segment. Development *126*, 4385–4394.
41. Pozzoli, O., Bosetti, A., Croci, L., Consalez, G.G., and Vetter, M.L. (2001). Xebf3 is a regulator of neuronal differentiation during primary neurogenesis in Xenopus. Dev. Biol. *233*, 495–512.
42. Prasad, B.C., Ye, B., Zackhary, R., Schrader, K., Seydoux, G., and Reed, R.R. (1998). unc-3, a gene required for axonal guidance in Caenorhabditis elegans, encodes a member of the O/E family of transcription factors. Development *125*, 1561–1568.
43. Hagman, J., Gutch, M.J., Lin, H., and Grosschedl, R. (1995). EBF contains a novel zinc coordination motif and multiple dimerization and transcriptional activation domains. EMBO J. *14*, 2907–2916.
44. Wang, S.S., Tsai, R.Y., and Reed, R.R. (1997). The characterization of the Olf-1/EBF-like HLH transcription factor family: implications in olfactory gene regulation and neuronal development. J. Neurosci. *17*, 4149–4158.
45. Wang, M.M., Tsai, R.Y., Schrader, K.A., and Reed, R.R. (1993). Genes encoding components of the olfactory signal transduction cascade contain a DNA binding site that may direct neuronal expression. Mol. Cell. Biol. *13*, 5805–5813.
46. Bellen, H.J., and Yamamoto, S. (2015). Morgan's legacy: fruit flies and the functional annotation of conserved genes. Cell *163*, 12–14.
47. Vervoort, M., Crozatier, M., Valle, D., and Vincent, A. (1999). The COE transcription factor Collier is a mediator of short-range Hedgehog-induced patterning of the Drosophila wing. Curr. Biol. *9*, 632–639.
48. Nagarkar-Jaiswal, S., Lee, P.T., Campbell, M.E., Chen, K., Anguiano-Zarate, S., Gutierrez, M.C., Busby, T., Lin, W.W., He, Y., Schulze, K.L., et al. (2015). A library of MiMICs allows tagging of genes and reversible, spatial and temporal knockdown of proteins in Drosophila. eLife *4*. http://dx.doi.org/10.7554/eLife.05338.
49. Venken, K.J., Schulze, K.L., Haelterman, N.A., Pan, H., He, Y., Evans-Holm, M., Carlson, J.W., Levis, R.W., Spradling, A.C., Hoskins, R.A., and Bellen, H.J. (2011). MiMIC: a highly versatile transposon insertion resource for engineering Drosophila melanogaster genes. Nat. Methods *8*, 737–743.
50. Diao, F., Ironfield, H., Luan, H., Diao, F., Shropshire, W.C., Ewer, J., Marr, E., Potter, C.J., Landgraf, M., and White, B.H. (2015). Plug-and-play genetic access to drosophila cell types using exchangeable exon cassettes. Cell Rep. *10*, 1410–1421.
51. Gnerer, J.P., Venken, K.J., and Dierick, H.A. (2015). Gene-specific cell labeling using MiMIC transposons. Nucleic Acids Res. *43*, e56.
52. Cook, R.K., Christensen, S.J., Deal, J.A., Coburn, R.A., Deal, M.E., Gresens, J.M., Kaufman, T.C., and Cook, K.R. (2012). The generation of chromosomal deletions to provide extensive coverage and subdivision of the Drosophila melanogaster genome. Genome Biol. *13*, R21.
53. Bischof, J., Sheils, E.M., Björklund, M., and Basler, K. (2014). Generation of a transgenic ORFeome library in Drosophila. Nat. Protoc. *9*, 1607–1620.
54. Firth, H.V., Richards, S.M., Bevan, A.P., Clayton, S., Corpas, M., Rajan, D., Van Vooren, S., Moreau, Y., Pettett, R.M., and Carter, N.P. (2009). DECIPHER: Database of Chromosomal Imbalance and Phenotype in Humans Using Ensembl Resources. Am. J. Hum. Genet. *84*, 524–533.
55. MacDonald, J.R., Ziman, R., Yuen, R.K., Feuk, L., and Scherer, S.W. (2014). The Database of Genomic Variants: a curated collection of structural variation in the human genome. Nucleic Acids Res. *42*, D986–D992.
56. Harms, F.L., Girisha, K.M., Hardigan, A.A., Kortüm, F., Shukla, A., Alawi, M., Dalal, A., Brady, L., Tarnopolsky, M., Bird, L.M., et al. (2016). Mutations in *EBF3* Disturb Transcriptional Profiles and Cause Intellectual Disability, Ataxia, and Facial Dysmorphism. Am. J. Hum. Genet. *100*, this issue, 117–127.

The American Journal of Human Genetics, Volume *100*

Supplemental Data

A Syndromic Neurodevelopmental Disorder Caused by De Novo Variants in *EBF3*

Hsiao-Tuan Chao, Mariska Davids, Elizabeth Burke, John G. Pappas, Jill A. Rosenfeld, Alexandra J. McCarty, Taylor Davis, Lynne Wolfe, Camilo Toro, Cynthia Tifft, Fan Xia, Nicholas Stong, Travis K. Johnson, Coral G. Warr, Undiagnosed Diseases Network, Shinya Yamamoto, David R. Adams, Thomas C. Markello, William A. Gahl, Hugo J. Bellen, Michael F. Wangler, and May Christine V. Malicdan

SUPPLEMENTAL NOTE

Proband #1 NIH Undiagnosed Diseases Program - *de novo EBF3* chr10: 131755588C>T (hg19): (NM_001005463.2: c.488G>A): p.Arg163Gln (R163Q)

Proband 1 is a seven-year old Pacific Islander male of Chinese and Japanese descent with expressive speech delay, mild dysmorphic facial features, hypotonia, global developmental delay, and genital hypoplasia.

His prenatal history was significant for maternal age of 33-years old and paternal age of 41-years old. Pregnancy was complicated by borderline hypertension and gestational diabetes, but responded to diet management. Mother reported that fetal movement was decreased compared to her previous pregnancy. There were no maternal exposures to drugs, alcohol, or trauma. Birth history was significant for delivery at 38-weeks gestation by repeat Caesarean section that was complicated by a loose nuchal cord wrapped once around the neck and a fractured clavicle. Birth weight: 7 lbs, 9 ozs; birth length: 20.5 inches; OFC: 36.2, Apgar scores: 7, 8.

Newborn exam was significant for micropenis and bilateral undescended testes. He was discharged in on day three of life. However, during the first 24-48 hours of life, he was reported to have episodes of choking, back arching, and a dusky appearance during breastfeeding that was followed by a period of decreased alertness. MRI brain was unremarkable for age per report. Sepsis evaluation was unrevealing. These episodes of choking and back arching during breastfeeding were attributed to gastro-esophageal reflux. His first-week of life was significant for reportedly absent crying and generalized hypotonia.

His first-year of life was notable for dysphagia, hypotonia, strabismus, and developmental delay. At nine-months of age he was only able to roll over and sit with support.

Therapies were initiated. By one-year of age, he achieved head control and dysphagia improved. An endocrine evaluation at this time confirmed testicular failure and he underwent bilateral orchiopexy. Repeat MRI of the brain at one-year of age was significant for mild prominence of the ventricles and sulci per report.

Genetics evaluation at 2-years of age was significant for dysmorphic facial features including myopathic facies with oval-shaped face, over-folding of the superior helices, bilateral epicanthal folds, short anterverted nostrils, and downturned corners of the mouth. He also had noticeable expressive language delay, generalized hypotonia, strabismus, and microphallus. Targeted biochemical and genetic testing was negative for Allan-Herndon-Dudley, Mowat-Wilson, Prader-Willi, and Rett syndromes. A complete metabolic evaluation was unremarkable.

At 7-years of age notable physical exam findings included astigmatism and hyperopia without retinal or optic nerve abnormalities, isolated right peroneal neuropathy of uncertain significance, and wide-based ataxic gait. Neuropyschiatric testing was significant for moderate fine motor delay and significant expressive, greater than receptive, language delays. His overall speech was limited verbally to approximately two words and approximately 100 signs. However, non-verbal receptive and comprehensive skills tested close to normal. Repeat MRI of the brain revealed bilateral small inferior posterior cerebellar lobes and posterior vermian hypoplasia with mildly abnormal ventricles and sulci.

Proband #2 Texas Children's Hospital - *de novo EBF3* chr10: 131755588C>T (hg19): (NM_001005463.2: c.488G>A): p.Arg163Gln (R163Q)

Proband 2 is a five-year old African-American female with expressive speech delay, mild dysmorphic facial features, hypotonia, and global developmental delay.

Her prenatal history was significant for maternal age of 43-years old and paternal age of 47-years old. Pregnancy was uncomplicated, but mother reports reduced fetal movements compared to her previous pregnancy. There were no maternal exposures to drugs, alcohol, or trauma. An amniocentesis was performed due to advanced maternal age and the results were normal. At 40-weeks gestation, oligohydramnios was noted on ultrasound but was absent on prior ultrasounds. Birth history was significant for delivery at 40-weeks gestation by induced vaginal delivery that was uncomplicated. Birth weight: 7 lbs, 6 ozs; birth length: 20 inches; OFC: 33.5 cm, Apgar scores: 8/8.

Newborn exam was unremarkable except for some noted compression of the left ear and left toes consistent with oligohydramnios. She was discharged in the first week of life.

Her first-year of life was notable for hypotonia, dysphagia, strabismus, and developmental delay. Hypotonia was noted within the first three months of life due to delayed head control and she continued to have poor head control at 9-10 months of age. She also had significant difficulty with control of oral secretions and was unable to swallow solid foods at 12-months of age. Therapies were initiated at 9-10 months of age.

Gross motor delays included the inability to sit without support until 12-months old, inability to roll over until 10-11 months old, and did not crawl independently until 18-months old. She achieved independent ambulation at 30-months old but continued to have a wide-based ataxic gait with frequent falls. Fine motor delays included the acquisition of raking grasp at 11-months old, pincer grasp at 30 months old, at 4-years of age she could assist with dressing

herself, and at 5-years of age she remains ambidextrous. Language delays included babbling at 11-months of age, first word at 11-months of age, and 2-3 word sentences at 4-years of age. Now at 5-years of age she is able to speak in short sentences with apraxic speech. Additionally, at 5-years of age she continues to have difficulty controlling her oral secretions and achieved bowel-control but not bladder-control. Her social behavior is noteworthy at 5-years of age for a short attention span, very curious and interactive, overly sociable with behavioral perseveration, and decreased awareness of boundaries or consequences.

Interestingly, she is reported to exhibit decreased pain sensitivity based absent signs of discomfort with vaccinations or falls until around 2-years of age and at 5-years of age is still described by mother as "tough to pain". She is also noted to have significantly decreased spontaneous facial expressions since birth that was most notably described as the inability to smile with emotion or on command. Physical exam at 5-years of age was notable for mild dysmorphic features including prominent forehead, triangular facies, facial hypotonia, overfolding of superior helices, epicanthus inversus, and abnormal palmar creases. Mild hypoplasia of the labia majora was noted.

Brain MRI was significant for a cleft in the superior cerebellar vermis, and reduced size of the middle cerebellar vermis. Cerebellar hemispheres were unremarkable.

Proband #3 NYU Langone Medical Center- *de novo EBF3* chr10: 131755588C>A (hg19): (NM_001005463.2: c.488G>T): p.Arg163Leu (R163L)

Proband 3 is a 3-year old Caucasian female of English, Irish, German, and Polish descent withexpressive speech delay, mild dysmorphic facial features, hypotonia, and global developmental delay.

Her prenatal history was significant for maternal age of 32-years old and paternal age of 31-years old. Pregnancy was uncomplicated and no invasive prenatal tests were performed. There were no reports of decreased fetal movements. There were no maternal exposures to drugs, alcohol, or trauma. Birth history was significant for delivery at 39-weeks gestation by Caesarean section due to breech position. Birth weight: 2.7 kg; Apgar scores: 7-9. Newborn exam was normal. The proband was discharged home within the first week of life.

Her first-year of life was notable for dysphagia, hypotonia, strabismus, and developmental delay. Occupational therapy was started at 3-weeks of age due to deficient latching and torticollis. At 3-months old she was diagnosed with gastroesophageal reflux (GERD) by upper gastrointestinal imaging series following an apparent life-threatening event and was treated with omeprazole. Developmental evaluation at 5-months of age was notable for significant hypotonia and global developmental delays. Gross motor delays include rolling over from prone to supine at 3-months of age but unable to roll over from supine to prone until 10-months of age. She was able to sit without support at 11-months of age and was able to put herself into a seated position at 13-months of age. By 12-months of age, she was commando crawling but did not pull to stand or cruise. Now at 30-months of age, she is ambulating independently with a wide-based waddling ataxic gait and occasionally drags her feet when fatigued. Language delays included babbling with consonant sounds but no words at 13-months of age. She has near normal receptive language with minimal expressive language (only has one or two words). She occasionally has flat affect with decreased facial expressions. Notably, parents report that she appears to exhibit increased tolerance to pain.

Clinical examination at 13-months old revealed head circumference at 20^{th}-%ile for length, 10^{th}-%ile for weight, difficulty controlling oral secretions, and torticollis. Heart murmur

was not heard. Spleen was not palpable, but liver was palpable. Mild dysmorphic features include a prominent occiput, triangular facies, metopic ridge, low set ears, down-slanting palpebral fissures, hypertelorism, beaked nose, facial hypotonia, small umbilical hernia, inverted nipples, small hemangioma on the back, tapered fingers, and small feet. She had stereotypic motor movements including bilateral writhing or piano tapping finger movements as well as simultaneous asynchronous knee and hip flexion with kicking movements of both feet. The stereotypies decreased in frequency at severity by 30-months of age.

At 2-years of age she had placement of myringotomy tubes due to conductive hearing loss after chronic otitis media with effusion. She also had recurrent urinary tract infections (UTI) and was diagnosed with urinary retention associated with incomplete bladder emptying and vesicoureteral reflux grade I. She was treated with Macrodantin for one year and had no further UTIs. At 30-months of age the GERD has resolved and torticollis is minimal.

Due to the motor stereotypies MRI of the brain and 24-hour ambulatory EEG studies were obtained at 13-months of age, both studies were unremarkable and appropriate for age. Chromosomal microarray, urine organic acids, plasma amino acids, carnitine levels, creatine kinase, acylcarnitine profile, Angelman/Prader Willi DNA methylation test and Pompe disease testing were unrevealing. Pelvic X-rays were normal. Follow-up MRI of the brain was unremarkable.

Table S1: Clinical Features of *EBF3* Probands

	Proband 1	**Proband 2**	**Proband 3**
Variant	Chr10: 131755588C>T (hg19): NM_001005463.2 c.488G>A p.Arg163Gln *de novo*	Chr10: 131755588C>T (hg19): NM_001005463.2 c.488G>A p.Arg163Gln *de novo*	Chr10: 131755588C>A (hg19) NM_001005463.2 c.488G>T p.Arg163Leu *de novo*
Age (evaluation)	7 year 4 month	5 years	3 year
Gender	Male	Female	Female
Ethnicity	Chinese and Japanese	African-American	English, Irish, German, and Polish
Prenatal findings	Reduced fetal movements	Oligohydramnios, reduced fetal movements	None
Birth growth parameters	Weight 7lbs 9oz Length 20.5 inches OFC 36.2	Weight 7lbs 9oz Length 20 inches OFC 33.5 cm	Weight 2.7 kg
Growth parameters at last exam	HT 109.7 cm (25-%ile) WT19.5 kg (25-%ile) OFC 52.5 (50-75-%ile)	WT 17.5 kg (41-%ile) HT 114.8 cm (91-%ile) OFC 51 cm (85-%ile)	WT 10-%ile HT 10-%ile OFC 20-%ile
Hypotonia	Resolved to proximal weakness about age 4 ½ years	Present since at least 3 months	Present since at least 3 months
Coordination	Ataxic wide based gait	Ataxic wide based gait, dysmetria	Ataxic wide based gait
Development	Expressive language and Fine motor delays (testing= 5 years, 10 months)	Global developmental delay	Global developmental delay
Speech delay	Severe expressive, 2-3 single words	Expressive delay, apraxic speech with short sentences at 5-years of age	Severe expressive, 1 word
Seizures	None	None	None
Ophthalmologic	Strabismus	Strabismus, surgical correction of extraocular movement dysfunction	Strabismus, surgical correction of extraocular movement dysfunction
Facial features	Oval shaped face, overfolding of superior helices, short anterverted nostrils, downturned corners of the mouth, hockey stick palmar creases	triangular shaped face, facial hypotonia, overfolding of superior helices, epicanthus inversus, abnormal palmar creases	Prominent occiput, triangular facies, metopic ridge, low set ears, down-slanting palpebral fissures, hypertelorism, beaked nose, facial hypotonia, small umbilical hernia, inverted nipples, small hemangioma on back, tapered fingers and small feet.
Facial Weakness	Present	Present	Present
Behavior	Stereotypic behaviors reported in the past. Full criteria were not formally evaluated.	Atypical social interactions – persistent eye gaze, perseveration, occasional flat affect	Motor stereotypies, occasional flat affect
Pain Insensitivity	None	Present	Present
MRI	Mild prominence of ventricles and sulci, decreased cerebellar hemisphere volume, vermian hypoplasia	Vermian hypoplasia	Normal
GU	Micropenis, testicular failure	Mild underdevelopment of the labia majora	Grade 1 reflux

Table S2: *EBF3* Variant Prediction Scores

	Proband 1+2	**Proband 3**
Variant	Chr10: 131755588C>T (hg19): NM_001005463.2 c.488G>A p.Arg163Gln *de novo*	Chr10: 131755588C>A (hg19) NM_001005463.2 c.488G>T p.Arg163Leu *de novo*
SIFT (Score)	0.01	0
SIFT (prediction)	Deleterious	Deleterious
PolyPhen-2 (Score)	0.994	0.993
PolyPhen(Prediction)	Probably Damaging	Probably damaging
Mutation Taster (Prediction)	Disease Causing	Disease Causing

Table S3: Sequencing Methods

	Proband 1	Proband 2	Proband 3
Sequencing laboratory	NIH Intramural Sequencing Center (NISC)	Baylor Genetics Laboratory	Baylor Genetics Laboratory
Sequencing type	Quad exome sequencing (Sanger sequencing of *EBF3* in proband, parents, and unaffected sibling)	Proband exome sequencing (Sanger sequencing of *EBF3* in proband and parents) (https://www.bcm.edu/research/medical-genetics-labs/index.cfm?PMID=21319)[1]	Proband exome sequencing (Sanger sequencing of *EBF3* in proband and parents) (https://www.bcm.edu/research/medical-genetics-labs/index.cfm?PMID=21319)[1]
Capture and library construction	Illumina TrueSeq capture kit	Biotin-labeled VCRome 2.1 in-solution Exome probes	Biotin-labeled VCRome 2.1 in-solution Exome probes
Sequencing platform	Illumina HiSeq2000	Illumina HiSeq2000	Illumina HiSeq2000
Sequence data aligned to human reference genome (hg19)	Novoaling (Novocraft Technologies, Selangor, Malaysia)	Human Genome Sequencing Center Mercury analysis pipeline (http://www.tinyurl.com/HGSC-Mercury)	Human Genome Sequencing Center Mercury analysis pipeline (http://www.tinyurl.com/HGSC-Mercury)
Analysis, sorting, and filtering of variants	Variants were analyzed, sorted and filtered with VarSifter and a graphical java tool to view, sort, and filter variants[2]. Variants were filtered based on allele frequencies in the NIH-UDP cohort[3-5] (<0.06) and variants were prioritized using CADD[6] and Exomiser[7]. Primers GAAACCAAGCAAGGCAAAAC and AATTCTCCAAACTGCCTTGG were used for the amplification of the region of genomic DNA around the mutation in *EBF3* (NM_001005463 c.488G>A; CADD 28.4). Sanger dideoxy sequencing of the PCR products was performed by Macrogen (Rockville, MD, USA). The sequences were aligned and analyzed using Sequencher v.5.0.1 (Gene Codes, Ann Arbor, MI, USA). Mutation interpretation analysis was conducted using Alamut 2.0 (Interactive Biosoftware, San Diego, CA, USA).	Variants were determined and called using the Atlas2 suite to produce a variant call file[8]. For the population comparisons we utilized data from the Exome Aggregation Consortium (ExAC), Cambridge, MA (URL: http://exac.broadinstitute.org) [November 2015] and Exome Variant Server, NHLBI GO Exome Sequencing Project (ESP), Seattle, WA (URL: http://evs.gs.washington.edu/EVS/) [November 2015].	Variants were determined and called using the Atlas2 suite to produce a variant call file[8]. For the population comparisons we utilized data from the Exome Aggregation Consortium (ExAC), Cambridge, MA (URL: http://exac.broadinstitute.org) [November 2015] and Exome Variant Server, NHLBI GO Exome Sequencing Project (ESP), Seattle, WA (URL: http://evs.gs.washington.edu/EVS/) [November 2015].

Table S4: Fly Genotypes Used in Study and Maintained at 21°C

Genotype	Allele	Source	Reference
w; kn^{col-1}/CyO*	Amorphic	Drosophila Genomics and Genetic Resources	http://www.ncbi.nlm.nih.gov/pubmed/10477305
kn^{1}/SM6a	Hypomorphic	Drosophila Genomics and Genetic Resources	http://www.ncbi.nlm.nih.gov/pubmed/10375526
w^{1118}; Df(2R)BSC429/CyO	Genomic deficiency allele including *knot* locus	Bloomington Drosophila Stock Center	http://www.ncbi.nlm.nih.gov/pubmed/22445104
M[UAS-kn.ORF.3xHA.GW]ZH-86Fb	Wildtype fly allele	FlyORF	http://www.ncbi.nlm.nih.gov/pubmed/24922270
y[1] w*; Mi{MIC}knot[MI15480]/SM6a	MiMIC	Bloomington Drosophila Stock Center	http://www.ncbi.nlm.nih.gov/pubmed/21985007
y[1] w; Mi{Trojan-GAL4.2}kn[MI15480-TG4.2]/SM6a*	T2A-GAL4	Bellen Lab	Line MI15480 was converted to *kn-T2A-GAL4* via recombinase mediated cassette exchange as previously described[9, 10].
y[1] w; M[UAS-EBF3.ORF.3xHA.GW]ZH-86Fb/TM3, Sb Ser*	UAS	Bellen Lab	Transgenic flies were generated by ϕC31-mediated transgenesis with the pUASattB vector and integrated into the same *86Fb* (chromosome 3) docking sites to minimize position effects on transgene expression[11-13].
y[1] w; M[UAS-EBF3-p.Arg163Gln.ORF.3xHA.GW]ZH-86Fb/TM3, Sb Ser*	UAS	Bellen Lab	Transgenic flies were generated by ϕC31-mediated transgenesis with the pUASattB vector and integrated into the same *86Fb* (chromosome 3) docking sites to minimize position effects on transgene expression[11-13].
y[1] w; M[UAS-EBF3-p.Arg163Leu.ORF.3xHA.GW]ZH-86Fb/TM3, Sb Ser*	UAS	Bellen Lab	Transgenic flies were generated by ϕC31-mediated transgenesis and with the pUASattB vector integrated into the same *86Fb* (chromosome 3) docking sites to minimize position effects on transgene expression[11-13].

Table S5: Antibodies Used in Study

Antibody	Dilution	Source	Reference
rat anti-Elav-7E8A10	1:50	Developmental Studies Hybridoma Bank	http://www.ncbi.nlm.nih.gov/pubmed/8033205
Mouse anti-HA	1:200	Covance (Catalog #MMS-101P)	n/a
DAPI	1:100	Thermo-Fisher (Catalog #D1306)	n/a
Donkey anti-rat Alexa 647	1:300	Jackson ImmunoResearch (Catalog #712-605-153)	n/a
Donkey anti-mouse Cy3	1:300	Jackson ImmunoResearch (Catalog #715-165-150)	n/a

Table S6: Oligonucleotide Pairs Used in Study

Purpose	Forward or Reverse	Sequence
Site directed mutagenesis for EBF3 p.Arg163Gln	Forward	5'-CACGAGATCATGTGCAGTCAATGCTGTGACAAGAAAAGTTG-3'
Site directed mutagenesis for EBF3 p.Arg163Gln	Reverse	5'-AACTTTTCTTGTCACAGCATTGACTGCACATGATCTCGTGG-3'
Site directed mutagenesis for EBF3 p.Arg163Leu	Forward	5'-ATGTGCAGCCTGTGCTGTGAC-3'
Site directed mutagenesis for EBF3 p.Arg163Leu	Reverse	5'-GATCTCGTGGGTCAGCAG-3'
Concatamerized COE binding sequence	Forward	5'-CTAGCTCTCAGGATTCCCCAGGGAGGGGACACTCTCAGGATTCCCCA GGGAGGGGACACTCTCAGGATTCCCCAGGGAGGGGACACCTAGGC-3'
Concatamerized COE binding sequence	Reverse	5'-TCGAGCCTAGGTGTCCCCTCCCTGGGGAATCCTGAGAGTGTCCCC TCCCTGGGGAATCCTGAGAGTGTCCCCTCCCTGGGGAATCCTGAGAG-3'
Site directed mutagenesis for EBF3 deletion of the Zn^{2+} finger COE motif (ΔCOE)	Forward	5'-GGCAATAGAAACGAAACGCCC-3'
Site directed mutagenesis for EBF3 deletion of the Zn^{2+} finger COE motif (ΔCOE)	Reverse	5'-GGTCAGCAGCACACGGCA-3'

SUPPLEMENTAL REFERENCES

[1] Lupski, J. R. et al. Exome sequencing resolves apparent incidental findings and reveals further complexity of SH3TC2 variant alleles causing Charcot-Marie-Tooth neuropathy. Genome Med 5, 57 (2013).

[2] Teer, J. K., Green, E. D., Mullikin, J. C. & Biesecker, L. G. VarSifter: visualizing and analyzing exome-scale sequence variation data on a desktop computer. Bioinformatics 28, 599-600 (2012).

[3] Markello, T. C. et al. Recombination mapping using Boolean logic and high-density SNP genotyping for exome sequence filtering. Mol Genet Metab 105, 382-9 (2012).

[4] Gahl, W. A. et al. The National Institutes of Health Undiagnosed Diseases Program: insights into rare diseases. Genet Med 14, 51-9 (2012).

[5] Gahl, W. A. & Tifft, C. J. The NIH Undiagnosed Diseases Program: lessons learned. Jama 305, 1904-5 (2011).

[6] Marchler-Bauer, A. et al. CDD: a Conserved Domain Database for the functional annotation of proteins. Nucleic Acids Res 39, D225-9 (2011).

[7] Smedley, D. et al. Next-generation diagnostics and disease-gene discovery with the Exomiser. Nat Protoc 10, 2004-15 (2015).

[8] Danecek, P. et al. The variant call format and VCFtools. Bioinformatics 27, 2156-8 (2011).

[9] Diao, F. et al. Plug-and-play genetic access to drosophila cell types using exchangeable exon cassettes. Cell Rep 10, 1410-21 (2015).

[10] Gnerer, J. P., Venken, K. J. & Dierick, H. A. Gene-specific cell labeling using MiMIC transposons. Nucleic Acids Res 43, e56 (2015).

[11] Groth, A. C., Fish, M., Nusse, R. & Calos, M. P. Construction of transgenic Drosophila by using the site-specific integrase from phage phiC31. Genetics 166, 1775-82 (2004).

[12] Horn, C. & Handler, A. M. Site-specific genomic targeting in Drosophila. Proc Natl Acad Sci U S A 102, 12483-8 (2005).

[13] Venken, K. J., He, Y., Hoskins, R. A. & Bellen, H. J. P[acman]: a BAC transgenic platform for targeted insertion of large DNA fragments in D. melanogaster. Science 314, 1747-51 (2006).